BMC Microbiology

RESEARCH

Open Access

Salinity-induced virulence alteration of *Aeromonas hydrophila* isolated from *Scatophagus argus*: insights from transcriptomic profiling and phenotypic characterization

Yuan Sun[1,2†], Lingyun Hao[1,3†], Jianbing Liang[1], Shiyang Ye[1] and Maoliang Su[1*]

Abstract

Background The emerging foodborne pathogen, *Aeromonas hydrophila*, co-infects humans and animals, especially fish, threatening aquacultural production and public health. Previously, we found that *Scatophagus argus*, a widely cultivated fish species with high economic value, exhibited enhanced growth but increased susceptibility to *A. hydrophila* infection under freshwater conditions compared to seawater conditions. However, the exact mechanisms involved remain unclear.

Results Our study demonstrated that the enhanced virulence of *A. hydrophila* 201416, isolated from *S. argus*, in response to increasing salinity was associated with altered quorum sensing-related gene expression and regulated behaviors. Results from virulence assays incorporating phenotypic characterization indicated that elevated salinity levels (from 0 to 35‰) significantly hindered *Ah*201416 infection of *S. argus*. This trend correlated with increased biofilm mass and swimming motility, yet was inversely related to bacterial growth. RNA-sequencing and quantitative reverse transcriptional PCR analysis confirmed significant upregulation of genes related to flagellar assembly (*flgB*, *flgH*, *flgC*, *flgI*, *flhA*, and *fliA*), bacterial secretion (*HlyD* and *Ahh1*), and quorum sensing (*AhyR*, *LuxO*, and *LuxE*) of *Ah*201416 in response to elevated salinity. These findings suggested that increased salinity not only enhanced the virulence of *Ah*201416 but also bolstered the resistance of *S. argus*, thereby mitigating its susceptibility.

Conclusions This study provides deeper insights into the microbial risks associated with *A. hydrophila* in aquacultural production, which is critical to developing effective prevention and control strategies and ensuring a safe seafood supply.

Clinical trial number Not applicable.

†Yuan Sun and Lingyun Hao contributed equally to this work.

*Correspondence:
Maoliang Su
mlsu@szu.edu.cn

Full list of author information is available at the end of the article

Keywords Food safety, *Aeromonas hydrophila*, *Scatophagus argus*, Salinity fluctuation, Bacterial virulence, Quorum sensing regulated behaviors, RNA-sequencing

Introduction

Food safety is paramount within the food industry [1]. Despite the implementation of comprehensive disinfection strategies, pathogenic microbes continue to frequently breach food safety barriers, leading to outbreaks of illness [2, 3]. According to the World Health Organization, approximately 600 million individuals worldwide are infected with foodborne pathogens, leading to approximately 420,000 fatalities annually [4]. These data highlight the importance of controlling pathogens in food production to enhance food safety and protect consumers from illness [1]. Effective management and control of pathogens in cultured organisms are crucial in aquaculture, in which these aquatic products have the potential to transmit pathogens to humans, leading to significant infections.

The gram-negative bacterium *Aeromonas hydrophila* is widely distributed in aquatic environments and can infect a wide range of aquatic animals [5], including numerous cultivated fish species and leading to *Aeromonas* septicemia [6, 7]. *A. hydrophila* exhibits a broad range of salinity tolerance, and different strains have been isolated from fresh, brackish, and saline environments [8]. Freshwater ecosystems have been identified as significant reservoirs of *A. hydrophila*, posing notable risks to fish health and aquatic food safety [9]. Contaminated aquatic products can act as vehicles for transmitting this pathogen to human beings, potentially leading to severe infections, especially among elderly individuals and those with compromised immune systems. Consequently, *A. hydrophila* has been recognized as an emerging foodborne pathogen that presents a substantial threat to public health.

Current strategies for mitigating *A. hydrophila* infections predominantly involve the use of antibiotics; however, this practice has resulted in multiple forms of resistance within the pathogen and has raised concerns regarding environmental and food safety [10]. It is imperative to develop innovative and sustainable strategies that target bacterial virulence, rather than relying exclusively on direct bactericidal effects. *A. hydrophila* produces a wide array of virulence factors, such as cytotoxic enterotoxin, hemolysin, protease, and lipase. This bacterium employs polar flagella for motility in liquid environments and lateral flagella for swarming. These adaptations facilitate niche exploration, evasion of unfavorable environmental conditions, and enhanced antimicrobial resistance [11]. Forming biofilm is another crucial virulence factor for initial attachment and subsequent establishment within host tissues, contributing to disease causation and resistance against antimicrobial compounds produced by the host. Quorum sensing, a conserved and widely distributed mechanism in bacteria that coordinates collective behaviors based on population density, primarily regulates the production of virulence factors and other associated biological processes as described above [12]. Several studies have demonstrated that interfering with bacterial quorum sensing and biofilm formation can significantly inhibit or even eliminate their virulence. This suggests that these infection mechanisms may serve as promising targets for the development of novel disease management strategies [13, 14, 15]. To date, several environmental factors, including salinity, ammonium levels, pH, and temperature, have been shown to impact the virulence of *A. hydrophila*; however, a comprehensive understanding of the underlying mechanisms remains elusive [16, 17]. Further investigation into the mechanisms by which *A. hydrophila* modulates these virulence-associated behaviors and regulates corresponding gene expression in response to diverse environmental stimuli will facilitate the development of sustainable approaches to combat this pathogen.

Coastal aquaculture accounts for more than 50% of the total aquaculture production and has emerged as a prominent form of fish farming, particularly in developing nations [18, 19]. The salinity levels of coastal areas often experience significant fluctuations due to global climate change, evaporation, and ocean currents. In certain coastal areas, such as South China, the salinity can decrease from 35‰ to below 10‰ during the rainy season [20, 21]. Therefore, salinity is arguably one of the most crucial environmental factors that impact coastal aquaculture. It not only affects the growth and metabolism of cultivated species in these areas but also significantly influences their resistance to pathogens [22, 23, 24, 25]. The fish *Scatophagus argus* is primarily distributed in the coastal areas of the Indo-Pacific region [26]. In recent years, owing to its considerable economic value, there has been a notable rise in large-scale aquaculture operations involving this species along the coastlines of South China [27, 28]. The variation of salinity throughout the life cycle of *S. argus* in its natural habitat has been estimated to range from 0 to 35‰ [29]. Previously, Jahid et al. [30] demonstrated that salinity and culture duration significantly influence the production of virulence enzymes and quorum sensing regulated phenotypes in *A. hydrophila in vitro*, highlighting the critical role of these environmental factors in shaping bacterial virulence. In our previous study, we found that *S. argus* exhibits enhanced growth in freshwater and brackish water conditions, accompanied by a suppression of its immune response, which resulted

in increased susceptibility to *A. hydrophila* infection compared to seawater conditions [31]. This susceptibility is associated with the decline of body resistance under stress. However, the extent and manner in which salinity fluctuation influences *A. hydrophila* infection of *S. argus*, as well as the underlying molecular mechanisms, remain to be elucidated. A comprehensive evaluation of fish susceptibility and bacterial virulence under varying salinity conditions can reduce breeding risks and enhance the development of food safety control strategies.

In this study, individuals of *S. argus* were initially acclimated to different salinity conditions: freshwater (salt-free, 0‰), brackish water (10, 15, 20, and 25‰), and seawater (35‰), respectively. The fish from each group were individually injected with *A. hydrophila* cells that had been pre-cultured under the same salinity conditions as the host fish, and then monitored for 96 h to analyze mortality rates, thereby investigating the impact of salinity on bacterial virulence. Furthermore, we conducted phenotypic characterization of *A. hydrophila*, including bacterial growth, motility, and biofilm formation under varying salinity conditions. To elucidate the underlying molecular mechanisms involved in these processes, transcriptomic analysis was performed on *A. hydrophila* cells exposed to different salinity conditions. The expression of candidate genes related to motility, quorum sensing, and secretory pathways was validated using quantitative RT-PCR. This study aims to enhance our understanding of how salinity impacts *A. hydrophila* virulence and provide future guidance for appropriate aquatic farming practices and food safety.

Materials and methods

Experimental fish and bacterial cell preparation

The strain *A. hydrophila* (*Ah*201416), which was originally isolated from the liver of diseased *S. argus*, was obtained from Shanghai Ocean University. The bacterial cells were cultured in a modified Luria-Bertani (LB) medium containing 1.0 g tryptone, 0.5 g yeast extract, and 1.0 g NaCl per 100 mL of ddH_2O. A stock solution of NaCl (35‰) was prepared by dissolving 17.5 g of NaCl powder (Sangon Biotech, China) into 500 mL of H_2O and subsequently diluted with a sterile modified LB to obtain saline solutions with desired concentrations.

Table 1 The conversion coefficients of 0.7 (OD_{600}) and CFU/mL of *Ah*201416 cells cultured under different NaCl concentrations

The NaCl concentrations of bacterial culture	CFU/mL (OD_{600} = 0.7)
0‰	8.2×10^7
10‰	8.0×10^7
15‰	8.3×10^7
20‰	8.4×10^7
25‰	8.1×10^7
35‰	8.4×10^7

Healthy adult *S. argus* (with an average weight of 17.7 ± 2.3 g) was sourced from an aquatic farm in Zhanjiang City, Guangdong Province, China. The fish were acclimated in a temperature-controlled aquarium at 28 ± 1 ℃ for two weeks and fed twice daily with red worms. The aquarium was supplied with water at different salinity levels (0, 10, 15, 20, 25, and 35‰) prepared by natural sea salt (Red Sea company, Israel) and maintained through continuous aeration using a flow-through water system. No mortality was observed among the different salinity treatment groups during the two-week fish acclimation experiment. All experimental fish were confirmed to be vigorous and healthy, with no visible pathologies or parasitic infections detected prior to the virulence assay. All experiments followed the Guide for the Care and Use of Laboratory Animals (Ministry of Science and Technology of China, 2006) and were approved by the Animal Ethics Committee of Shenzhen University.

Virulence assay

The *Ah*201416 cells were incubated at 28 ℃ for 16–18 h in LB broth containing 10‰ NaCl. And this incubation process was repeated twice to ensure full resuscitation. Cells were subsequently harvested and inoculated into fresh LB medium at a ratio of 1:20 (vol/ vol). The fresh LB medium was supplemented with NaCl to achieve final concentrations of 0, 10, 15, 20, 25, and 35‰. The cultures were then incubated at 28 ℃ with shaking at a speed of 200 rpm for an additional period of 16–18 h. To determine the populations of each culture to ensure the same inoculum concentration for subsequent virulence assays, the relationship between the measured optical density at 600 nm (OD_{600}) and CFU/mL was determined. First, the OD_{600} of each culture was measured using the SparkControl™ Multimode Microplate Reader (Tecan, Switzerland), adjusted to 0.7, and plated onto LB agar plates, respectively. The population of the culture (CFU/mL) corresponding to 0.7 (OD_{600}) was calculated based on colony counting. The conversion coefficients of 0.7 (OD_{600}) and CFU/mL of *Ah*201416 cells were approximately 8.2×10^7 and documented in Table 1, demonstrating no significant variations across different salinity treatments. Cell morphology within the above-described salinity range had no significant difference, which has also been reported by several previous studies [32, 33].

Based on this, *Ah*201416 cells pre-cultured under each salinity were harvested and adjusted to concentrations ranging from 1×10^6 to 1×10^{10} CFU/mL with an interval of tenfold increment. Subsequently, a 100 μL bacterial suspension from each concentration was intraperitoneally injected into healthy *S. argus* cultivated under the same salinity levels. Control groups included individuals inoculated with an equal volume of saline solution at each concentration mentioned above. All fish were cultivated

in water with six different salinity levels prepared by natural sea salt (0, 10, 15, 20, 25, and 35‰; $n = 10$ individuals per group), accompanied by aeration through a flow-through water system maintained at 28 ± 1 ℃. Mortality of *S. argus* was recorded within 96 h post-inoculation. The virulence level was quantified as the lethal dose of 50% (LD_{50}) for *S. argus*, which was determined using the method described by Bennett [34]. The experiments were repeated three times.

Growth curves of *Ah*201416

The *Ah*201416 cells were cultured under the same conditions as described above and subsequently harvested. The fresh LB medium was supplemented with NaCl to achieve final concentrations of 0, 10, 15, 20, 25, and 35‰. A 200 µL aliquot of the harvested cells was pipetted into each well of a 96-well microplate. Bacterial growth was monitored every 2 h for 48 h by measuring the OD_{600}. Each treatment included six biological replicates, and the experiment was repeated three times.

Biofilm formation by *Ah*201416 under different salinities

The biofilm assay was conducted in 96-well plates following the protocol established by O'Toole et al. [35], with specific modifications implemented as necessary. In brief, *Ah*201416 cells were initially cultured overnight in an LB medium that contained NaCl at a concentration of 10‰. Following that, 50 µL of this bacterial culture was added to 150 µL of LB broth supplemented with NaCl to achieve final concentrations of 0, 10, 15, 20, 25, and 35‰, respectively. Subsequently, a volume of 200 µL from each inoculum was transferred into each well of a 96-well microplate (Corning Inc., Corning, NY). After static incubation at 25 ℃ for 20 h, each well was gently rinsed twice with a 0.85% saline solution, and the suspension cells were subsequently removed. The plates were dried at 60 ℃ for 2 h, followed by staining with a 1% (w/v in 96% ethanol) crystal violet solution (Spectrum Chemical Manufacturing Corp, New Brunswick, NJ) for 10 min at room temperature. Subsequently, the plates were washed three times with a 0.85% saline solution and then treated with 30% acetic acid to elute the dye bound to the cells in the biofilm. Finally, the plates were analyzed at OD_{590}. A blank medium without bacterial inoculation was used as a negative control. Each treatment included nine biological replicates, and the experiment was repeated three times.

Swimming motility assay

The swimming assay was conducted according to the previously described method with slight modifications [36]. Briefly, the bacterial overnight culture was adjusted to an optical density of 1.0 at a wavelength of 600 nm ($OD_{600} = 1.0$), and then a droplet of 1.5 µL was carefully placed in the center of a 9 cm-LB plate containing agar (0.3%, Sangon Biotech) supplemented with NaCl to achieve final concentrations of 0, 10, and 20‰, respectively. All plates were incubated at 25 ℃ for specific time intervals, including 10, 12, 16, 24, 32, and 36 h. At each designated time point, five replicates were photographed for each treatment, and this experiment was repeated three times.

Quantification of acyl-homoserine lactone production

The extraction of AHLs was performed as previously described [37], with some modifications. To quantify violacein production, *Ah*201416 cultures (250 mL) were grown in various concentrations of NaCl in modified LB broth at 28 ℃ for 18 h in a 1000 mL Erlenmeyer flask, after which the supernatant was collected by centrifugation at 10,000 × g for 10 min. The supernatant was then filter-sterilized using 0.22-mm filters (Titan, Shanghai, China). The supernatant was mixed with ethyl acetate at a 1:1 (v/v) ratio, vortexed vigorously for 1 min, and allowed to phase-separate. This liquid-liquid extraction step was repeated 3 times, and the organic phases were pooled. The combined organic phase was then concentrated to dryness using a rotary evaporator and reconstituted in a minimal volume of dimethyl sulfoxide (DMSO). Subsequently, an overnight culture of the bioreporter strain *Chromobacterium violaceum* CV026 was diluted with LB medium to an optical density of 0.1–0.2 at 595 nm. Aliquots of 90 µL of the diluted bacterial suspension were combined with 10 µL of filter-sterilized supernatant samples in a 96-well plate. The plate was incubated at 28 °C with orbital shaking (200 rpm) for 48 h. Following incubation, the mixed cultures were centrifuged at 15,000 × g for 5 min. The supernatant was discarded, and the violacein pigment was extracted by resuspending the pellet in 100 µL DMSO. After a final centrifugation (15,000 × g, 2 min), 100 µL of colored DMSO from each condition was measured using the SparkControl™ Multimode Microplate Reader at 550 nm. Six replicates were carried out for each treatment, and this experiment was repeated three times.

Transcriptomic analysis

The *Ah*201416 cells were harvested after being cultured in an LB medium with different concentrations of NaCl for 18 h. Each experiment was performed in triplicate. Total RNA was extracted using the Eastep® Super Total RNA Extraction Kit (Promega, USA) following the manufacturer's instructions. 2 µg of RNA samples were used to construct an RNA-Seq library using a Truseq™ RNA sample prep Kit for Illumina (NEB, USA). The indexed libraries were subsequently pooled and subjected to sequencing on the HiSeq™ 2500 platform (Illumina, USA), which generated 2*150-bp

paired-end reads. The reference genome used was *A. hydrophila* (ASM1602687v1). Gene annotation was conducted using the NR, SwissProt, PFAM, GO, KEGG, and STRING databases. The FPKM values of the differentially expressed genes (DEGs) were normalized through $\log_2$ transformation and median-centered. Genes with an adjusted *P*-value < 0.001 and $\log_2|\text{fold-change}| \geq 1$ were considered statistically significant [38]. GO and KEGG enrichment analyses were performed to identify the biological functions of DEGs. All sequencing and bioinformatics analysis were performed by the Shanghai OE Biotech Co., Ltd, Shanghai, China.

cDNA preparation and RT-qPCR validation

The integrity of the RNA extracted from *Ah*201416 cells cultured in the medium containing 0, 10, and 20‰ NaCl for 18 h was assessed through gel electrophoresis. Each group was performed in triplicate. The concentration of RNA was quantified using a Nanodrop-2000 spectrophotometer (Thermo Scientific, USA). After DNase treatment, 1 μg of total RNA was subjected to reverse transcription to generate single-strand cDNA using an Eastep® RT Master Mix Kit (Promega, USA), according to the manufacturer's instructions. The resulting cDNA was then stored at – 20 ℃.

Primer-BLAST (https://www.ncbi.nlm.nih.gov/tools/primer-blast/index.cgi) was used to design specific primers for analyzing candidate genes by RT-PCR. The 16 S rRNA gene was selected as the internal reference [39]. All primer sequences employed in this study are listed in Table 2. The qPCR was performed using SYBR Premix Ex Taq II (Takara, Japan) and a Quant Studio™ 3 Real-Time PCR System (Thermo Scientific, USA). The reaction program was set as follows: 95 ℃ for 34 s; 40 cycles of 95 ℃ for 5 s and 60 ℃ for 30 s; 95 ℃ for 15 s; 60 ℃ for 1 min; and 95 ℃ for 15 s (final dissociation) [40]. The data were collected at 60 ℃. Each experiment was conducted in triplicate. Changes in gene expression levels were analyzed using the $2^{-\Delta\Delta Ct}$ method [41]. The relative quantification of transcripts was presented as fold-change compared to the expression value of the control group. Each experiment was set up with three biological replicates, each of which included three technical replicates.

Table 2 Primers used in RT-qPCR

Gene	Primer sequence	Amplified fragment in base pairs
flgB	F: TGTCCAGCAACATTGCCAAC	125 bp
	R: ATGCTTCTCACTGGTCGTGG	
flgH	F: AGTCTGCAGGGCAACATCTC	181 bp
	R: CATTGGCCACCTTCTGGGAT	
flgC	F: AACACGGTAGCCAGCAACAT	244 bp
	R: CCATGTTGACGTTGGGCTTG	
flgI	F: AGCCCAAGATCAAGGACGTG	172 bp
	R: GCATAGACCCGACCATCCAG	
flhA	F: TCCAGGTTGTCGCGGATATG	196 bp
	R: ACGAGCAGAAAGACCTGAGC	
fliA	F: GATCCCGGCGTAGGTTTCAA	208 bp
	R: CCAAGCGTACTTGCGTCATC	
HlyD	F: CCGAGCAGCAGAAGGATGAC	214 bp
	R: TTGGTGATGATGCCGTCCTG	
Ahh1	F: CTCTTCGTCCAGCGAGATCC	206 bp
	R: TCTACCTCAACGTCAACCGC	
AhyI	F: ATGATGCAGGTCAGTTCGCT	163 bp
	R: TCAGCTGTGCCCAGGATTAC	
AhyR	F: TTCAACCAGTGCCCAGACTC	162 bp
	R: CATCACGTCAAGACTGCCCT	
LuxO	F: ATGATGCGATAGACCGCCTG	171 bp
	R: CGCCTTCGACTTTCTGACCA	
LuxE	F: GAACCCACCTGTTCCACCAT	216 bp
	R: CGGCTTCACCTTCATGGTCT	
16 S rRNA	F: TAATACCGCATACGCCCTAC	164 bp
	R: ACCGTGTCTCAGTTCCAGTG	

flgB: gene encoding flagellar basal body rod protein; *flgH*: gene encoding flagellar basal body L-ring protein; *flgC*: gene encoding flagellar basal body rod protein; *flgI*: gene encoding flagellar basal body P-ring protein; *flhA*: gene encoding flagellar biosynthesis protein; *fliA*: gene encoding RNA polymerase sigma factor; *HlyD*: gene encoding HlyD family secretion protein; *Ahh1*: gene encoding hemolysin; *AhyI*: gene encoding acyl-homoserine-lactone synthase; *AhyR*: gene encoding transcriptional activator protein and LuxR family transcriptional regulator; *LuxO*: gene encoding quorum-sensing sigma-54 dependent transcriptional regulator; *LuxE*: gene encoding acyl-protein synthetase. F: forward, R: reverse

Statistical analysis

The statistical analyses were conducted using SPSS 20.0 software (SPSS Inc., Chicago, IL, USA). Data obtained from the biofilm formation assay, motility test, and gene expression analysis were subjected to One-way analysis of variance (ANOVA) with the least significant difference (LSD) test for pairwise comparisons between the salinity treatment group and the salt-free control group. Subsequently, Fisher's post-hoc tests were conducted to further evaluate the differences. The level of statistical significance was set at $P < 0.05$ (* $p < 0.05$, ** $p < 0.01$, *** $p < 0.001$).

Results

Effects of salinity on the strain *Ah*201416 virulence

The impact of salinity on the virulence of *Ah*201416 on *S. argus* was investigated by determining the LD_{50} for cells pre-cultured at different salinities. Overall, bacterial virulence was significantly higher in cells grown under hyposaline conditions compared to those grown under hypersaline conditions (Table 3). At 96 h post-infection (hpi), the mortality rate of *S. argus* acclimated to six different salinities gradually decreased when inoculated with *Ah*201416 cells that were pre-cultured in medium containing accompanied NaCl concentrations, with LD_{50} values of 1.3×10^6, 6.3×10^6, 9.8×10^7, 1.1×10^8, 2.8×10^8,

Table 3 LD_{50} of the strain *Ah*201416

NaCl concentrations of bacterial culture (‰)	LD_{50}(CFU/mL)of *S. argus* under different salinities					
	0‰	10‰	15‰	20‰	25‰	35‰
0	1.3×10^{6}					
10		6.3×10^{6}				
15			9.8×10^{7}			
20				1.1×10^{8}		
25					2.8×10^{8}	
35						6.9×10^{8}

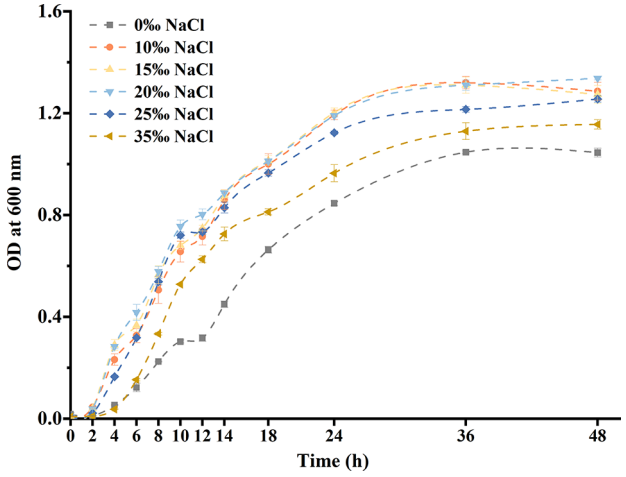

Fig. 1 Growth curves of *Ah*201416 in LB broth supplemented with different concentrations of NaCl. Experiments were performed in sextuplicate and repeated three times. The data were presented as the mean ± standard error (SE). The growth curves of *Ah*201416 were illustrated using distinct colored lines under various NaCl conditions, including 0, 10, 15, 20, 25, and 35‰

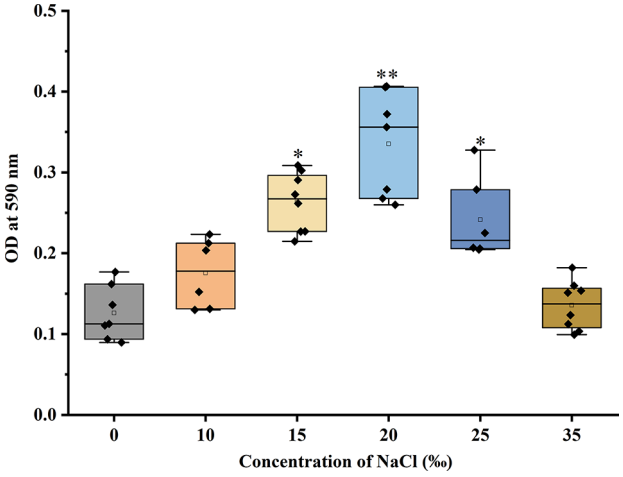

Fig. 2 Effects of salinity on *Ah*201416 biofilm formation. The experiments were performed in nonuplicate and repeated three times. The data obtained from the salinity treatment group and the salt-free control group were analyzed using ANOVA, followed by Fisher's post-hoc test for multiple comparisons. The data were presented as the mean ± SE. * $P<0.05$; ** $P<0.01$

and 6.9×10^{8} CFU/mL, respectively. The increase in NaCl concentration from 0 to 35‰ resulted in a 530.8-fold reduction in the pathogenicity of *Ah*201416, indicating that *Ah*201416 exhibited lower virulence under hypersaline conditions (e.g. 35‰) compared to hyposaline conditions.

Growth of the strain *Ah*201416 under different salinities

The initial step of investigating the impact of salinity on bacterial virulence involved conducting a growth curve assay to assess the fitness of *Ah*201416 under varying salinity conditions. As shown in Fig. 1, *Ah*201416 exhibited optimal growth in LB medium with 10, 15, and 20‰ NaCl, with no significant differences observed among these groups at different time points. The OD_{600} values within these groups ranged from 0.7 to 0.8 at 12 hpi, increased to approximately 1.1–1.2 at 24 hpi, and reached a plateau around 36 hpi with OD_{600} values of approximately 1.2–1.3. In contrast, 25‰ and 35‰ NaCl exhibited a slight inhibitory effect on pathogen growth. Conversely, the absence of salt supplementation significantly hindered and delayed pathogen growth, with the highest OD_{600} reading observed at 36 hpi being significantly lower than that of the other treatments ($P<0.01$). These findings indicated that the optimal salinity range for *Ah*201416 was 10–20‰, while concentrations outside this range might have a negative impact on bacterial fitness.

Biofilm formation of the strain *Ah*201416 under salinity stress

Biofilm formation is a well-established factor strongly associated with the virulence of numerous pathogenic bacteria. In this study, we investigated the biofilm formation ability of *Ah*201416 at varying salt concentrations. Overall, it was observed that the biofilm formation of *Ah*201416 was enhanced with an increase in salinity within the range of 0–20‰ (Fig. 2). The biofilm formation of *Ah*201416 was significantly higher under the condition of 20‰ NaCl, showing an approximate increase of 62.4%, 47.7%, and 59.5% compared to the levels of 0, 10, and 35‰ groups respectively. Furthermore, *Ah*201416 cultured in LB medium containing 25‰ NaCl exhibited a significant reduction of approximately 27.8% in biofilm formation compared to that with 20‰ NaCl ($P<0.05$), and it was similar to cells cultured under the condition

of 15‰ NaCl ($P > 0.05$). Notably, the biofilm formation of *Ah*201416 was significantly inhibited when the salinity level increased from 20 to 35‰, compared to the level at 20‰ ($P < 0.05$). Our results indicated that salinity could impact the ability of *Ah*201416 to develop a biofilm, potentially altering bacterial virulence.

Swimming motility of the strain *Ah*201416 under salinity stress

Motility is crucial in bacterial infection, enabling the bacterium to explore favorable niches and migrate within host tissues. The effects of salinity on *Ah*201416 swimming motility were illustrated in Fig. 3, with cells exhibiting their highest migration distance on swimming plates with 10‰ NaCl. At 12, 16, 24, 32, and 36 hpi, the swimming distance was approximately 10.4 mm, 16.3 mm, 31.9 mm, 48.7 mm, and 55.9 mm, respectively. In contrast, the swimming distance of cells on plates with 20‰ NaCl at these time points of 12, 16, 24, 32, and 36 hpi was measured as follows: 8.9 mm, 13.8 mm, 25.9 mm, 41.1 mm, and 48.7 mm, respectively. Cells in salt-free conditions moved the slowest, with a swimming distance of only approximately 3.0 mm at 36 hpi. These results indicated that both 10‰ and 20‰ NaCl could

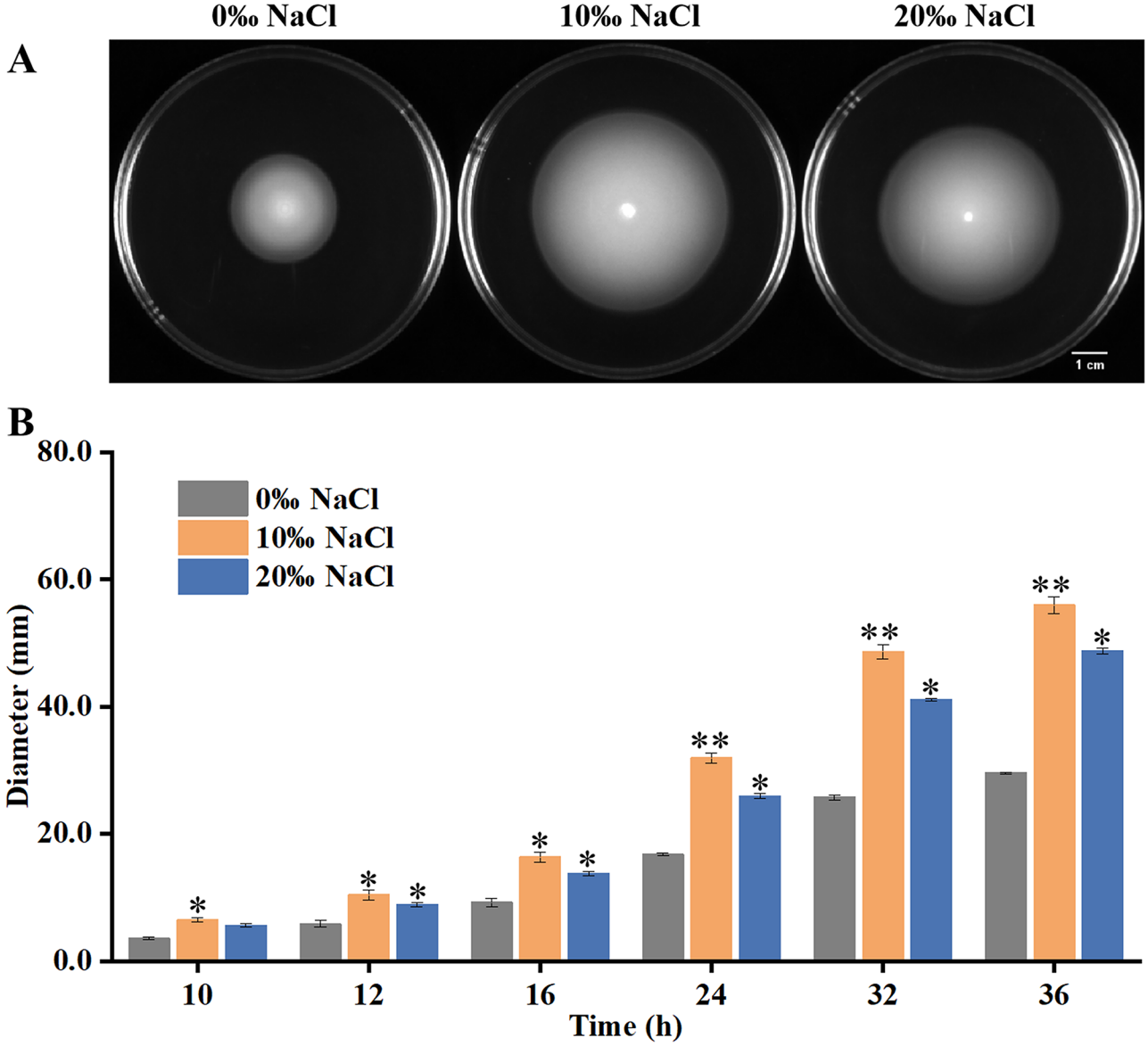

Fig. 3 Effects of salinity on *Ah*201416 swimming motility. Experiments were performed in quintuplicate and repeated three times. The illustrations show (**A**) representative images of *Ah*201416 swimming plates supplemented with different concentrations of NaCl captured at 36 hpi, and (**B**) the average distance covered by *Ah*201416 cells during different time intervals. The data obtained from the salinity treatment group and the salt-free control group were analyzed using ANOVA, followed by Fisher's post-hoc test for multiple comparisons. The data were presented as the mean ± SE. * $P < 0.05$; ** $P < 0.01$

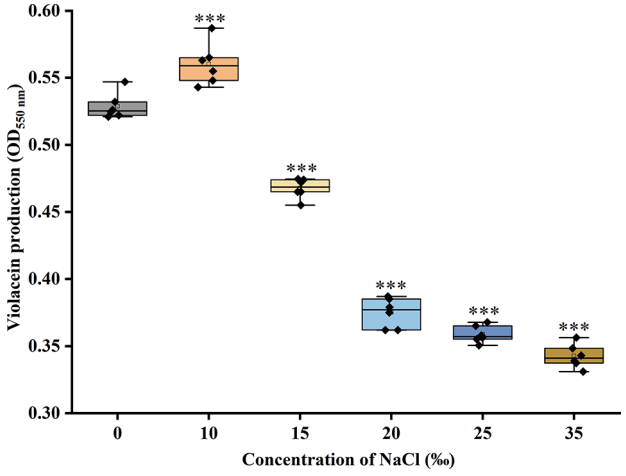

Fig. 4 Violacein production in *Ah*201416 under different salinity conditions. The data obtained from the salinity treatment group and the salt-free control group were analyzed using ANOVA, followed by Fisher's post-hoc test for multiple comparisons. The data were presented as the mean ± SE. *** $P < 0.001$

significantly enhance the motility of *Ah*201416 compared to the salt-free condition, especially under a salinity level of 10‰.

AHL quorum sensing of the strain *Ah*201416 under salinity stress

AHL quorum sensing has been found to regulate *A. hydrophila* virulence in fish [42]. In this study, we quantified the AHL production of *Ah*201416 at varying salt concentrations using the bioreporter strain *Chromobacterium violaceum* CV026. Increasing salinity from 0‰ to 10‰ significantly increased AHL production, and salinity from 10‰ to 35‰, followed by a significant decrease in AHL production (Fig. 4, $P < 0.001$). The AHL production of *Ah*201416 was significantly higher under the condition of 10‰ NaCl, showing an approximate increase of 5.9%, 19.8%, 49.4%, 56.1%, and 63.6% compared to the levels of 0, 15, 20, 25, and 35‰ NaCl groups, respectively ($P < 0.001$). Furthermore, *Ah*201416 cultured in LB medium ranging from 20 to 35‰ NaCl exhibited a significant reduction of approximately 32.2% in AHL production compared to that with 0‰ NaCl ($P < 0.001$). The current findings indicated that salinity could impact AHL quorum sensing, potentially relating to biofilm formation, motility, and bacterial virulence.

Functional analysis of DEGs in the strain *Ah*201416 under different salinities

The present study acquired 44.637 GB of Clean Data (sequencing data after quality control), with an average amount of Clean Data per sample being 4.960 GB. The high-quality sequence reads and assembly provided a solid foundation for all subsequent analyses.

Table 4 Summary statistics of *A. hydrophila* transcriptome annotation information

Category	Number of genes	Percentage (%)
Annotated in all databases	1,783	42.1
Annotated in at least one database	4,231	99.9
Annotated in GO	2,724	64.3
Annotated in KEGG	2,605	61.5
Annotated in NR	4,231	99.9
Annotated in PFAM	3,571	84.3
Annotated in STRING	3,271	77.3
Annotated in SWISS-PROT	2,848	67.3

GO: Gene Ontology; KEGG: Kyoto Encyclopedia of Genes and Genomes; NR: NCBI Non-Redundant Protein Sequences; PFAM: Protein Family; STRING: Protein-Protein Interaction Networks and Functional Enrichment Analysis; SWISS-PROT: A Manually Annotated and Reviewed Protein Sequence Database

After obtaining the spliced transcript, it is necessary to perform functional annotation to obtain gene functional information. A total of 2,605 genes were functionally annotated using the KEGG database (Table 4). The four species with the highest alignment rates between annotated genes and unknown genes all belonged to *Aeromonas* sp., including *A. hydrophila* (62.9%), *Aeromonas* sp. (32.0%), *A. hydrophila* subsp. (ATCC 7966) (1.9%), and *A. dhakensis* (0.5%) (Fig. 5A). The assembled genes were subjected to BLASTP searches against the GO, COG, and KEGG databases. A total of 2,724 genes were assigned to 41 subcategories of GO terms within the three main categories: 'biological process (BP)', 'cellular component (CC)', and 'molecular function (MF)' (Fig. 5B). The most notable subcategories included those associated with 'response to stimulus', 'locomotion', and 'toxin activity'. Regarding COG annotation, out of the 2,718 genes that mapped to the COG database, they were clustered into 21 categories which showed enrichment in two specific categories: 'Cell motility' (55) and 'Signal transduction mechanisms' (224) (Fig. 5C).

KEGG is a comprehensive database integrating genomic, chemical, and system function information. One notable feature of KEGG is its ability to link gene catalogs generated by RNA-Seq to higher-level system functions at the cellular, species, and ecosystem levels. To gain further insights into the biological pathways involved in the response to salinity stress in the strain *Ah*201416, we utilized KEGG pathway tools for mapping the gene sequences. The classification of 2,751 genes was accomplished across 25 specific pathways (Fig. 5D). The KEGG analysis revealed that similar to the results of GO analysis and COG classification, 'Cellular Processes' and 'Environmental Information Processing' were identified as important classifications. These categories encompassed sub-classifications like 'Cell growth and death', 'Cell motility', 'Cellular community', and

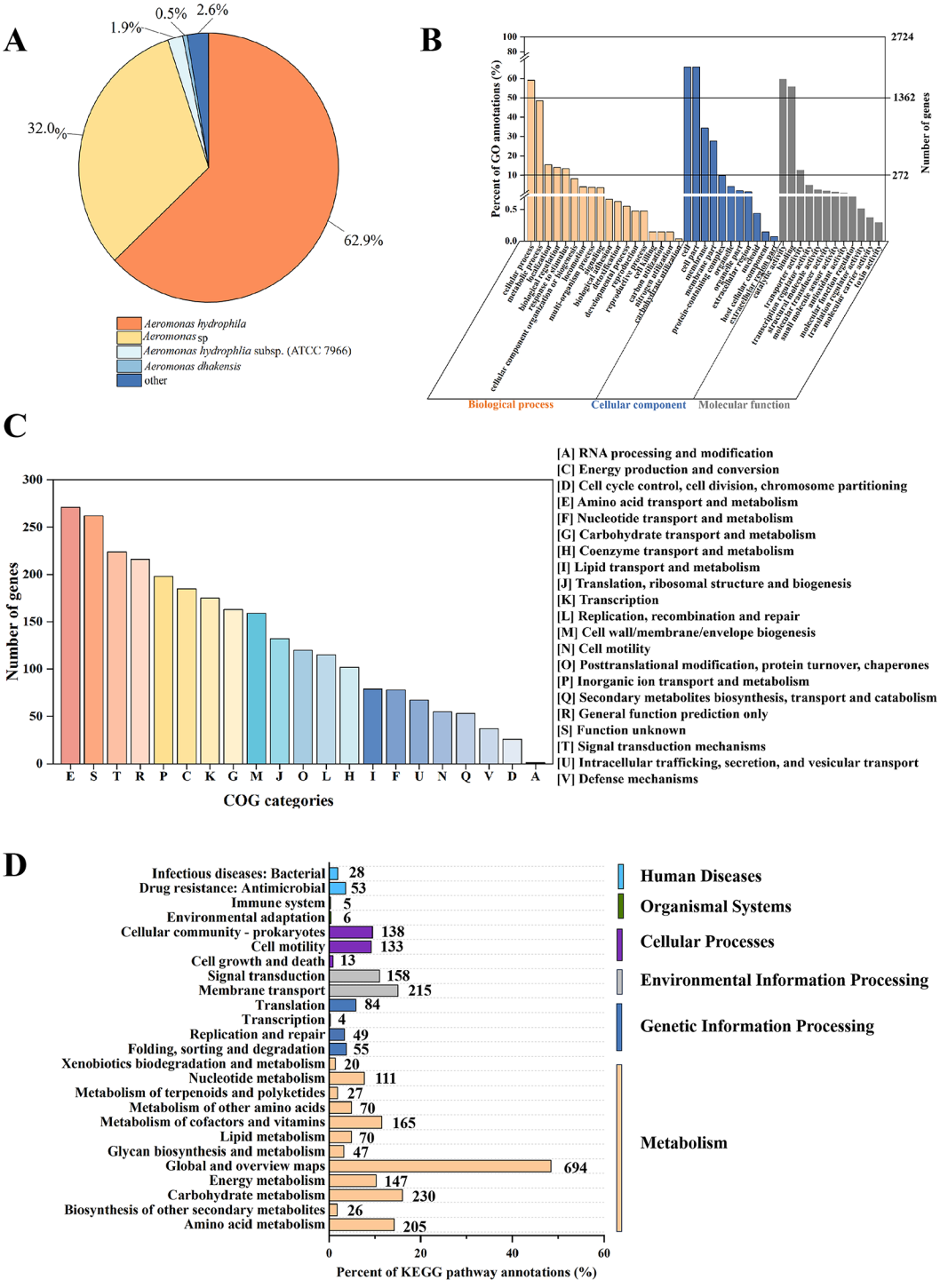

Fig. 5 (**A**) Characteristic of homology search for Illumina sequences against the NR database. Species distribution is shown as the percentage of the total homologous sequences using a cutoff *E*-value threshold (< 1e-6). All teleost proteins in the NCBI NR database were used in the homology search, and the best hits of the sequences were extracted for analysis. (**B**) GO annotation of genes. The results were summarized into three main categories: biological process, cellular component, and molecular function. (**C**) COG function classification of genes. (**D**) KEGG pathway (level 2) annotation of genes

'Signal transduction'. These annotations provided valuable resources for obtaining a more profound comprehension of specific biological functions demonstrated by the *Ah*201416 strain under different salinity stresses.

In comparison to the control group (0‰), a total of 1,376 up-regulated and 1,643 down-regulated DEGs were identified in the 10‰ group. Among these DEGs, *Ah*201416 exhibited significant differential expression

with 235 up-regulated and 324 down-regulated DEGs at a significance level of $P < 0.05$ and $\log_2|\text{fold-change}| \geq 1$ (Fig. 6). Similarly, upon comparing the control and 20‰ groups, a total of 3,028 DEGs were identified with 1,405 up-regulated and 1,623 down-regulated DEGs. Additionally, there were significantly expressed genes observed between the control and the 20‰ groups with a total of 544 DEGs consisting of 250 up-regulated and 294 down-regulated genes ($P < 0.05$ and $\log_2|\text{fold-change}| \geq 1$).

The DEGs in the *Ah*201416 strain under salinity stress were annotated and categorized into the KEGG databases to investigate the potential functions. The significantly altered KEGG pathways ($P < 0.05$) included Flagellar assembly (ko02040), Quorum sensing (ko02024), Bacterial secretion system (ko03070), Two-component system (ko02020), Bacterial chemotaxis (ko02030), Biofilm formation (ko05111, ko02025 and ko02026), and Biosynthesis of secondary metabolites (ko01110) (Fig. 7). Furthermore, KEGG pathway enrichment analysis revealed that the motility and secretion processes of *Ah*201416 were significantly affected by exposure to fluctuating salinity levels.

RT-qPCR validation of candidate genes in the flagellar assembly, bacterial secretion, and quorum sensing pathways

Based on the results of transcriptomic analysis, 12 candidate genes were selected for RT-qPCR validation, considering a $\log_2|\text{fold-change}| \geq 1$. The overall trend of gene expression change is consistent between the transcriptomic and RT-qPCR analyses, supporting the validity of the transcriptomic sequencing results. The expression levels of gene encoding flagellar basal body rod protein (*flgB*), flagellar basal body rod protein (*flgC*), flagellar biosynthesis protein (*flhA*), and RNA polymerase sigma factor (*fliA*) showed significantly upregulated by 19.8-fold, 14.5-fold, 9.9-fold, and 17.2-fold, respectively under a salinity of 20‰ compared to those under a salinity of 0‰ as depicted in Fig. 8. On the other hand, the expression levels of gene encoding flagellar basal body L-ring protein (*flgH*) and flagellar basal body P-ring protein (*flgI*) showed relatively lower induction at a NaCl concentration of 20‰, with upregulation by approximately 3.3-fold and 1.6-fold, respectively. A similar trend was observed with the gene encoding HlyD family secretion protein (*hlyD*) and hemolysin (*Ahh1*), which encode a component of the type I secretion system and a pore-forming toxin, respectively. These two genes exhibited an up-regulation of 3.3-fold and 2.1-fold in response to a salinity concentration

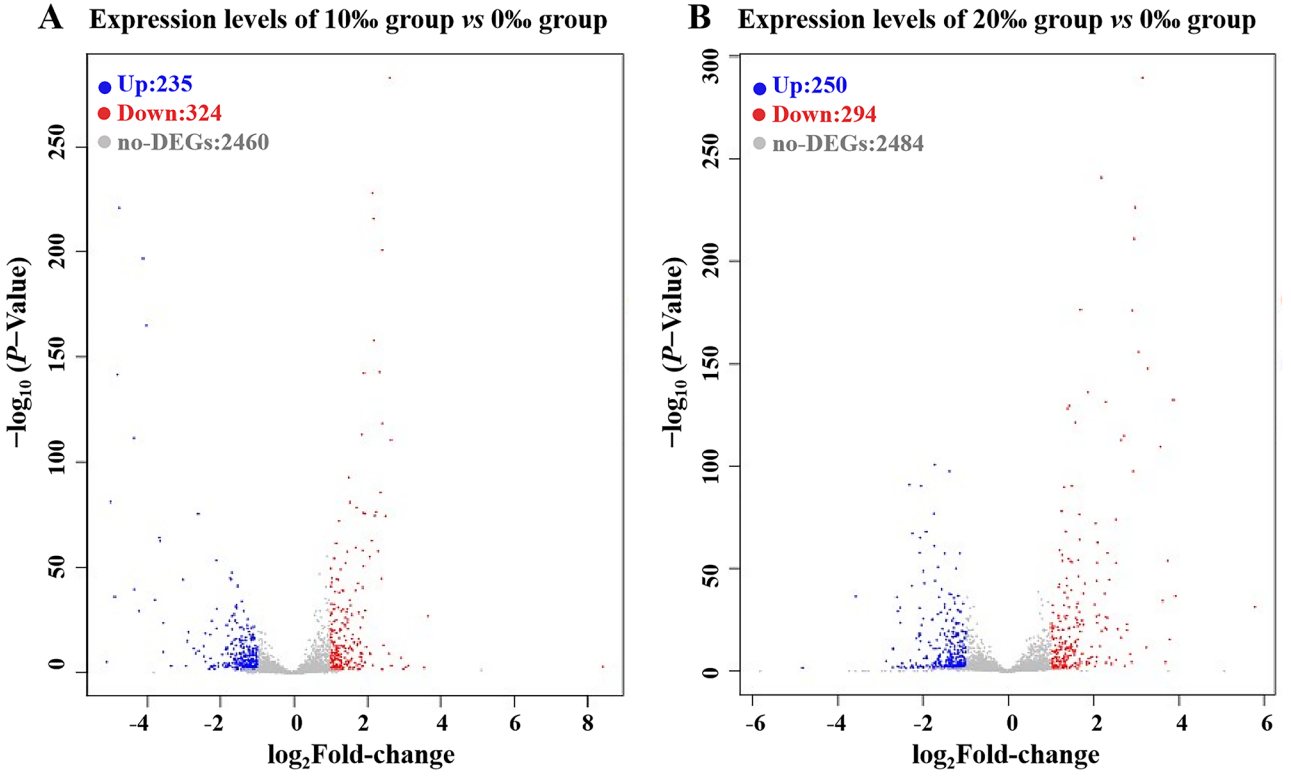

Fig. 6 Differentially expressed genes in (**A**) 10‰ vs. 0‰ and (**B**) 20‰ vs. 0‰. The horizontal axis represents the logarithmic fold change, while the vertical axis represents statistical test values. A higher number of points on either side of the horizontal axis indicates a greater upregulation or downregulation in gene expression

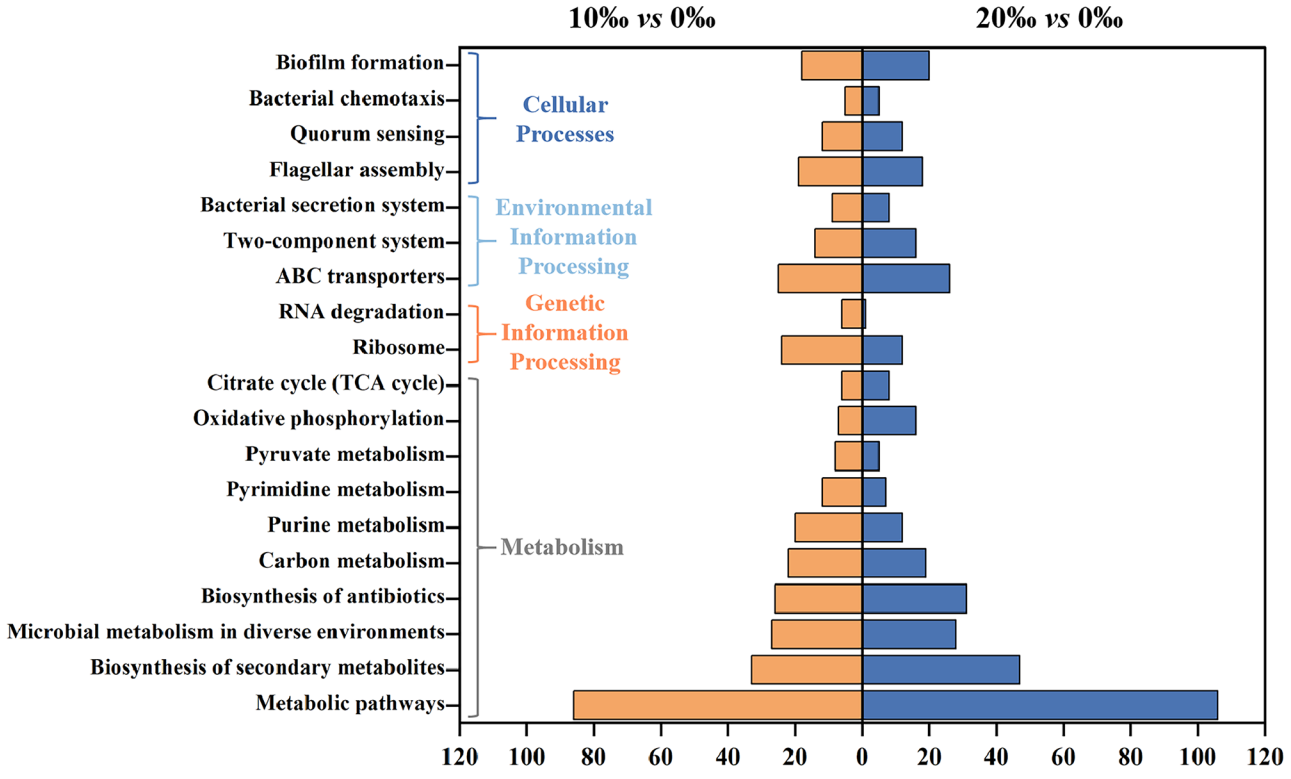

Fig. 7 KEGG pathway (level 3) classification for DEGs. Orange bars represent KEGG pathway classification for DEGs identified by comparing the 10‰ and 0‰ NaCl treatments. Blue bars represent KEGG pathway classification for DEGs by comparing the 20‰ and 0‰ NaCl treatments

of 10‰, and an up-regulation of 14.9-fold and 3.4-fold in response to a salinity concentration of 20‰ compared to the salt-free group (Fig. 9A). Among the three other genes involved in quorum sensing, namely gene encoding transcriptional activator protein and LuxR family transcriptional regulator (*AhyR*), quorum-sensing sigma-54 dependent transcriptional regulator (*LuxO*), and acyl-protein synthetase (*LuxE*), their highest upregulation was observed in 10‰ group as opposed to either the 0 or 20‰ groups. The gene encoding acyl-homoserine-lactone synthase (*AhyI*) was the only gene that demonstrated downregulation with increasing salinity levels (Fig. 9B). Collectively, these results suggested that salinity impacted *Ah*201416 virulence by modulating the expression of genes associated with multiple virulence-associated pathways.

Discussion

Salinity plays a crucial role in the interaction between aquatic animals and bacterial pathogens, which significantly impacts the outcomes of disease outbreaks [43, 44]. The facultative pathogen *A. hydrophila*, frequently isolated from diverse aquatic foods, exhibits a remarkable ability to orchestrate gene expression cascades to optimize its fitness and selectively produce virulence factors when necessary. Upon entering an animal host, one of the primary environmental changes encountered by the bacterium is a significant alteration in osmotic pressure compared to its free-living phase. This alteration may potentially serve as a signal for triggering the expression of virulence genes, enabling evasion of host immunity and initiation of infection [45, 46]. In a pilot study conducted by Lu et al. [31], it was discovered that salinity exerts an influence on various immune responses of *S. argus* upon infection with *A. hydrophila*. However, specific impacts of salinity on the pathogen's lifestyle remain unknown. In this study, the LD_{50} of *Ah*201416 exhibited an increase when it was pre-cultured under progressively higher salinity conditions before inoculation, indicating that lower salinity levels potentially promoted bacterial virulence compared to higher salinity. The observed phenomenon aligns with the pathogen's lifestyle since the salinity level in the host's digestive system typically ranges around 5‰, whereas in environmental waters it can vary from 0 to 35‰ [24, 29]. The decrease in salinity encountered by bacteria on entry into a host's internal milieu may enhance the virulence of the pathogen and enhance its invasiveness. Similar findings have also been reported in other bacterial pathogens. For instance, Barca et al. [47] demonstrated that genes related to involved in energy production, nutrient transport, and assimilation, as well as antibiotic resistance, were significantly upregulated in *Photobacterium damselae* subsp. *damselae* under elevated salinity mimicking a free-living lifestyle.

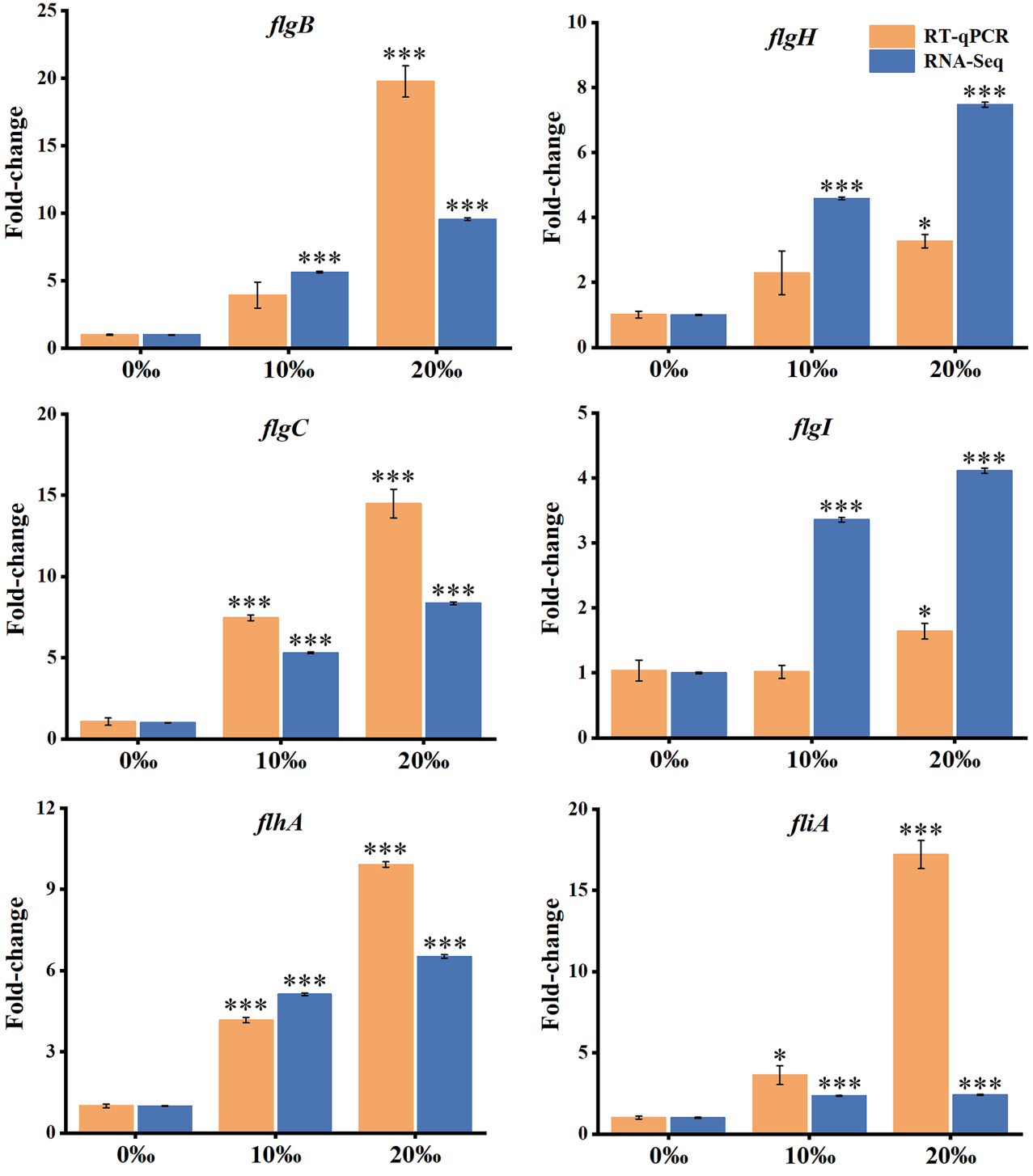

Fig. 8 Changes in relative expression levels of the six DEGs associated with flagellar assembly based on RNA-Seq (blue) and RT-qPCR (orange) analyses under different salinity treatments. Experiments were performed in triplicate. The data obtained from the salinity treatment group and the salt-free control group were analyzed using ANOVA, followed by Fisher's post-hoc test for multiple comparisons. The data were presented as the mean ± SE. * $P < 0.05$; ** $P < 0.01$; *** $P < 0.001$

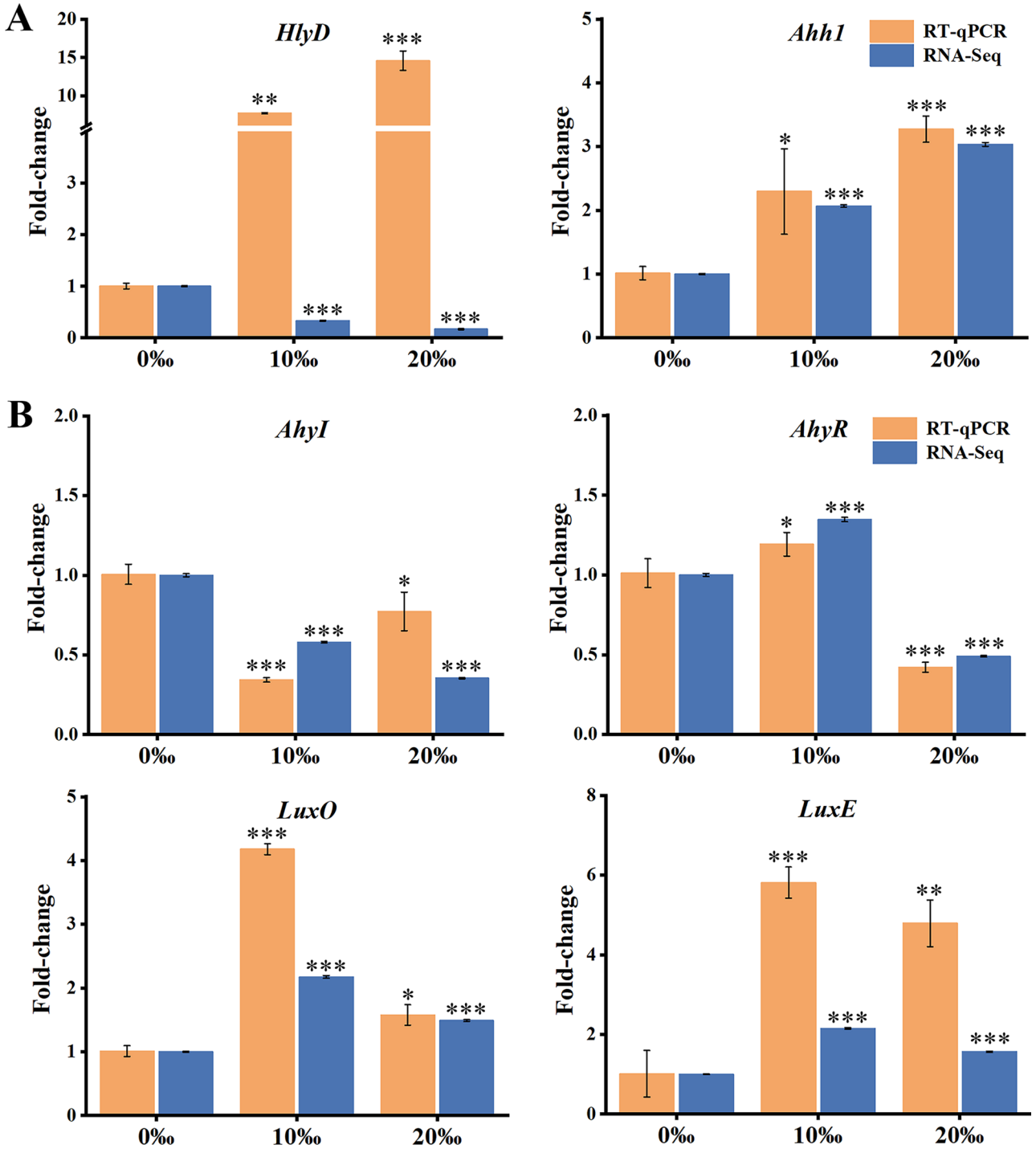

Fig. 9 Changes in relative expression levels of the six DEGs associated with bacterial secretion (**A**) and quorum sensing (**B**) based on RNA-Seq (blue) and RT-qPCR (orange) analyses under different salinity treatments. Experiments were performed in triplicate. The data obtained from the salinity treatment group and the salt-free control group were analyzed using ANOVA, followed by Fisher's post-hoc test for multiple comparisons. The data were presented as the mean ± SE. * $P < 0.05$; ** $P < 0.01$; *** $P < 0.001$

Conversely, there was an increased expression of virulence genes in the pathogen under hyposaline conditions that mimic those encountered in the host. Therefore, the results obtained from the virulence assay possibly further corroborate and elucidate the findings of our previous study, demonstrating that variations in environmental salinity have dual effects on both host susceptibility and *A. hydrophila* virulence.

Although different species and strains may vary in their susceptibility to osmotic stress, the *Aeromonas*

spp. generally exhibit a wide tolerance range for salinity, with optimal growth occurring at 10–20‰ [33, 48, 49, 50]. In our study, the results of the growth assay were aligned with these findings. Considering that the LD_{50} of *Ah*201416 cells pre-cultured in a medium containing 35‰ NaCl was almost 530-fold higher than those pre-cultured in a salt-free medium, we hypothesized that the disparity in infection capability was more likely attributed to variations in virulence behaviors rather than growth. Therefore, we investigated key infection-associated phenotypes such as biofilm formation and swimming under different salt conditions.

Biofilm formation is extensively investigated as a virulence determinant in *A. hydrophila*, enhancing its resistance to antimicrobial compounds and other stresses, thereby contributing to pathogen adaptation and persistence [51]. In this study, we demonstrated a gradual increase in biofilm biomass in *A. hydrophila* when cultured with increasing salinity ranging from 0 to 20‰. However, supplementation of 25‰ NaCl resulted in a decrease in biofilm mass comparable to that of the 15‰ group, but a slight inhibition of bacterial growth was observed in the group exposed to 25‰ NaCl. This observation is consistent with previous findings reported by Jahid et al. [30]. A positive correlation was observed between increasing biofilm formation and NaCl concentration in hyposaline conditions, whereas this trend was reversed under hypersaline conditions. However, it is important to note that the hyposaline conditions employed in their research ranged from 1 to 2.5‰, which were approximately ten times lower than those in our study. This discrepancy might be attributed to variations in strains and experimental settings, such as the contact surface employed between the two studies. The relationship between salinity and biofilm formation is quite controversial. For example, the formation of biofilms was significantly enhanced with the increase of NaCl concentrations in *Staphylococcus aureus*, whereas this phenomenon was reversed in *E. coli* K-12 [52]. Since biofilm formation is a multifactorial process and highly sensitive to environmental conditions, various factors such as secreted polysaccharides and adhesins, cultural media, cell age, strains, physical properties of the contact surface, and incubation time can all impact bacteria's capability of forming biofilms. Further investigation into how salinity affects *A. hydrophila*'s production of components such as lipopolysaccharides and adhesins will provide more insights into the observed phenomena.

A typical biofilm formation process in *Aeromonas* includes attachment, microcolony formation, maturation, and dispersion [12]. Among these, the initial attachment step has been studied most, and several bacterial structural factors have been reported to be involved, including flagella, lipopolysaccharides (LPS), and Mg^{2+} transporters. In contrast, genetic determinants involved in the later phases have been poorly studied. According to a review study conducted by Emilie et al. [12], nearly 20 genes are known to participate in biofilm formation, with *CheA*, *VgrG*, *MgtE*, *MinD*, *BioD*, *Psl*, *Pel*, *AhyR*, *AhyI*, *Mcp*, *LuxQ*, *LuxU*, *LuxO*, *LuxR*, *LuxE*, *LitR*, *QseB*, *QseC* as positive regulators. In align with these, our data shows *MinD*, *LuxO*, *LuxE*, *LuxR*, and *Mcp* were upregulated either under 10‰ or 20‰ salinity, compared to the salt-free control group, whereas *MgtE*, *BioD*, and *AhyI* showed a reversed trend (Table 5). These findings suggest that biofilm formation is influenced by multifaceted factors, and the precise molecular mechanisms underlying these regulatory pathways warrant further investigation. It is worth noting that enhanced biofilm formation often positively correlates with bacterial virulence [53, 54]. Nevertheless, exceptions should not be overlooked. The mutant *A. hydrophila* TM90, in which a gene encoding

Table 5 Known biofilm-related genes and DEGs from our transcriptomic data

Phases of Aeromonas biofilm development	Known biofilm-related genes	DEGs from our transcriptomic data
Attachment	Genes involved in substratum properties, nutrients availability (*BioD*), chemical environment, polar flagellum, lateral flagella, chemotaxis system (*CheA*), LPS, O-antigen, surface α-glucan (*Psl*, *Pel*), Mg^{2+} transporter (*MgtE*), cytoskeleton (*MinD*), type VI secretion system (*VgrG*) *	*MinD*↑, *MgtE*↓, *BioD*↓
Microcolony formation	Genes involved in lateral flagella, type IV pili, and the cytoskeleton	
Maturation	Genes involved in EPS (proteins, polysaccharides, extracellular DNA, lipids), quorum sensing AI-1 (*AhyR*, *AhyI*), c-di-GMP (GGDEF domains) *	*AhyI*↓
Dispersion	Genes involved in nutrient limitation, polar flagellum (*Mcp*), quorum sensing AI-2 (*LuxQ*, *LuxU*, *LuxO*, *LuxR*, *LuxE*, *LitR*) *, quorum sensing AI-3 (*QseB*, *QseC*) *, c-di-GMP (EAL domains) *	*LuxO*↑, *LuxE*↑, *LuxR*↑, *Mcp*↑

*: putative effectors; DEGs: Differentially expressed genes; *CheA*: gene encoding chemotaxis protein CheA; *VgrG*: gene encoding type VI secretion system effector VgrG; *MgtE*: gene encoding Mg^{2+} transporter; *MinD*: gene encoding septum site-determining protein MinD; *BioD*: gene encoding dethiobiotin synthase; *Psl*: gene encoding polysaccharide synthesis locus; *Pel*: gene encoding Pel extracellular polysaccharide locus; *AhyR*: gene encoding transcriptional activator protein and LuxR family transcriptional regulator; *AhyI*: gene encoding acyl-homoserine-lactone synthase; *LuxQ*: gene encoding quorum-sensing autoinducer 2 sensor kinase/phosphatase LuxQ; *LuxU*: gene encoding quorum-sensing phosphorelay protein LuxU; *LuxO*: gene encoding quorum-sensing sigma-54 dependent transcriptional regulator; *LuxR*: gene encoding LuxR family transcriptional regulator; *LuxE*: gene encoding acyl-protein synthetase; *LitR*: gene encoding quorum sensing transcriptional regulator; *QseB*: gene encoding quorum sensing response regulator transcription factor QseB; *QseC*: gene encoding quorum sensing histidine kinase QseC; *Mcp*: gene encoding methyl-accepting chemotaxis protein

oligopeptidase F (*pepF*) was disrupted, exhibited significantly increased adhesion to HEp-2 cells and biofilm formation, resulting in highly attenuated virulence in zebrafish compared to the wild-type strain [55]. Considering the profound immunosuppressive effects of hyposaline stress on *S. argus*, the increased biofilm formation of *Ah*201416 may be more crucial for pathogen survival and persistence rather than its virulence.

The motility of bacteria is widely recognized as essential for exploring different ecological niches, evading unfavorable environments, and biofilm formation, and thus contributing to the virulence of numerous foodborne bacterial pathogens [56]. As expected, the swimming ability of *Ah*201416 was affected by salinity. The bacterium exhibited a significantly higher migration rate in the 10‰ group compared to the 20‰ group, which was positively correlated with increased virulence and enhanced growth observed under the 10‰ condition. In contrast, *Ah*201416 displayed the suboptimal growth in salt-free LB medium and demonstrated slower movement on the swimming plates without salt; however, it exhibited the highest infectivity at this concentration. The observed phenomenon might be attributed to the potent immunosuppressive effects of freshwater on *S. argus* [31]. Similarly, Li et al. [57] discovered that hyposaline stress increased oyster mortality caused by *Vibrio* infection by inducing immune dysregulation, rather than exerting direct impacts on pathogen growth or virulence. The outcome of any infection is influenced not only by the virulence of the pathogen and environmental conditions but also by the host's immune status. A comprehensive assessment of the impact of environmental factors on bacterial virulence, as well as the influence of host resistance to infection, will significantly enhance our understanding of microbial risks. In turn, this would mitigate economic losses in aquaculture, prevent contamination from foodborne bacteria, and bolster food safety.

To further understand the molecular mechanisms underlying the difference in *A. hydrophila* biofilm formation and motility under varying salinity conditions, we conducted a transcriptomic analysis of *Ah*201416 cells cultured in a medium containing 0, 10, and 20‰ NaCl. As expected, DEGs between 0 and 10‰ groups were predominantly clustered in the pathways related to motility, secretion, and quorum sensing. Subsequent RT-qPCR analysis revealed that all candidate genes involved in flagella assembly, except *flgI*, were upregulated in the 10‰ group compared to the 0‰ group. This finding was consistent with the observed migration phenotypes on plates. Interestingly, the levels of upregulation for these genes were even more pronounced in the 20‰ group compared to the 10‰ group, while simultaneously showing a decrease in swimming distance. The findings suggested that motility is a delicate process, and an excessive expression of the genes associated with flagella assembly might impede bacterial movement, as has been consistently reported [58]. In *A. hydrophila*, the regulation of polar flagella biogenesis involves a hierarchical network comprising at least 50 genes responsible for encoding structural subunits, regulatory proteins, and chemosensor machinery [59]. A previous study has demonstrated that mutants in the *fliM*, *flhA*, and *fliA* genes were incapable of producing polar flagella and also exhibited impaired adhesion capability and biofilm formation, suggesting a positive role of this filamentous adhesin in the process of biofilm formation [60]. Therefore, the increasing salinity-enhanced biofilm formation in *Ah*201416 might be partially attributed to the upregulation of genes associated with flagella assembly. However, further verification at the protein level is necessary.

In addition to biofilm and motility-associated genes, both the transcriptomic and RT-qPCR analyses also revealed an upregulation of genes involved in toxin secretion and quorum sensing pathways in the 10 and 20‰ groups, while no significant changes were seen in cyclic di-guanosine monophosphate (c-di-GMP) related ones. The *hlyD* gene encodes a component of the prototypical alpha-hemolysin (HlyA) bacterial type I secretion system, which, along with HlyB and TolC, forms a transmembrane channel through which HlyA is secreted [61]. The β pore-forming enterotoxin Ahh1 is a major virulence factor of *A. dhakensis* that causes perforation of the host cell membrane and subsequent cell death both in vivo and in vitro [62]. Whether the upregulation of these toxin-producing genes results in increased toxin biosynthesis necessitates additional experimental validation.

A. hydrophila is known to harbor 3 quorum-sensing (QS) systems, AI-1 (based on N-acylhomoserine lactone), -2 (based on S-ribosylhomocysteinase), -3 (based on QseB/Qsec-dependent autoinducer), respectively and all three pathways could affect biofilm and motility, and involve complex cross-talk and feedback regulation. *A. hydrophila* utilizes 3 QS systems to coordinate virulence and environmental adaptation. Existing studies have predominantly focused on the AI-1 system, which is directly linked to pathogenicity, while studies on the AI-2 and AI-3 systems remain limited in fish [63, 64]. Thus, in the present study, we mainly investigated AHL, a major signaling factor in the AI-1 system, and found that C4-AHL is one of the major QS signals produced through the AhyI/R system. Our transcriptomic and RT-qPCR data also revealed significant upregulation of *ahyR* under 10‰ than 20‰, which was consistent with the reporter bioassay results (Figs. 4 and 9B). Therefore, we speculated that increasing salinity from 10–35‰ probably decreased C4-AHL production, leading to downregulation of *Ahy* genes, resulting in decreased virulence. Compared to the AHL-based AI-1 system, AI-2 and AI-3 have been less

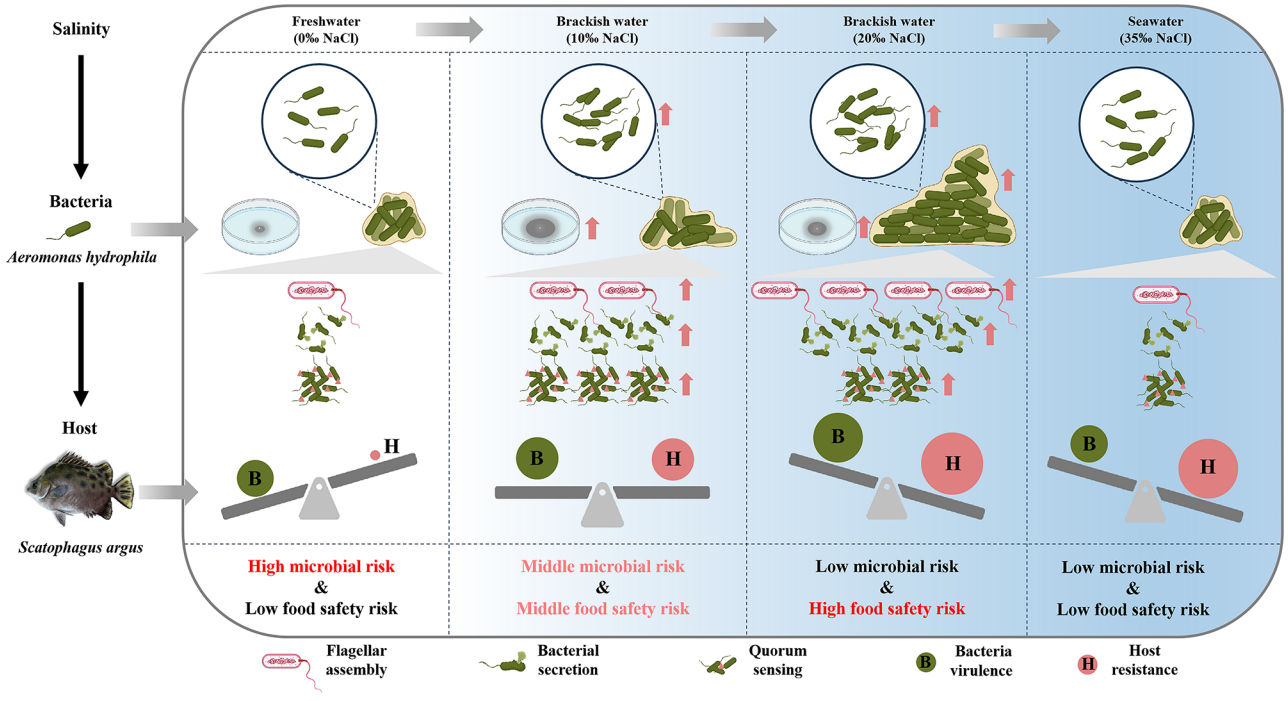

Fig. 10 Our investigation of salinity-induced virulence alteration of *Aeromonas hydrophila* isolated from *Scatophagus argus*

extensively documented. The impact of salinity on these signaling molecules, as well as the associated signaling pathways, and the extent to which these pathways contribute to virulence, warrant further investigation.

The secondary messenger c-di-GMP is another key signal that is known to be highly related to QS and bacterial virulence. In *Aeromonas*, c-di-GMP is believed to positively regulate biofilm formation while negatively affecting motility [12, 65]. However, in our transcriptomic data, we didn't identify any significant changes in c-di-GMP biosynthesis or degradation-related genes, such as *CsrA*, *CsrD*, *FleQ* (GGDEF domain-encoding genes), and *HapR* (EAL domain-encoding genes), suggesting salinity changes probably have minor effects on this pathway. Taken together, *A. hydrophila* virulence is regulated by several regulatory pathways, and its virulence is shaped not only by bacterial genetic determinants but also by host immunity. Our study emphasizes the role of salinity in bacterial virulence by influencing biofilm formation, swimming ability, and associated gene expression, and provides additional insights into the food ecology of *A. hydrophila*.

Conclusion

In summary, the virulence of *A. hydrophila* (*Ah*201416) isolated from *S. argus* was significantly enhanced by elevated salinity (from 0 to 20‰), as evidenced by increased growth, biofilm formation, motility, and expression of the virulence-associated genes. However, the susceptibility of *S. argus* decreased with increasing water salinity from 0 to 35‰, as indicated by an elevation in LD_{50} at 96 h post-infection. Our study demonstrated a significant microbial hazard posed by *A. hydrophila* to *S. argus* cultured in freshwater, as well as the potential risk this pathogen poses to food safety in brackish water due to its enhanced growth and biofilm formation capabilities (Fig. 10). From the perspective of breeding risk control and food safety, it is recommended to cultivate *S. argus* in seawater for commercial purposes. These findings suggest complex interactions among the pathogen, host, and environmental changes that collectively affect disease outcomes and food safety. Equal attention should be given to both bacterial virulence and host susceptibility, which may help to reduce the economic loss in aquaculture and the safety risks of aquatic food due to pathogenic bacterial infections.

Acknowledgements

The authors also warmly thank Professor Zhang Qinghua (College of Fisheries and Life Sciences, Shanghai Ocean University) for providing the original strains of Aeromonas hydrophila ***Ah***201416.

Author contributions

Conceptualization, M.S.; Data curation, L.H., and M.S.; Formal analysis, Y.S., and J.L.; Funding acquisition, Y.S., L.H., and M.S.; Investigation, Y.S.; Methodology, Y.S., and S.Y.; Project administration, M.S.; Resources, L.H., and M.S.; Software, Y.S.; Supervision, L.H., S.Y., and M.S.; Validation, Y.S., and J.L.; Writing-Original draft, Y.S.; Writing-Review and editing, L.H., and M.S. All authors have read and agreed to the published version of the manuscript.

Funding

This research was supported by the National Natural Science Foundation of China (41806177 and 42306177), the Natural Science Foundation of Guangdong Province, China (Grant No. 2025A1515010561), the Sustainable

Support Project from Shenzhen University (20231122143452002 and 20220811101028001), and the Scientific and Technical Innovation Council of Shenzhen (JCYJ20230808105807016).

Data availability

The transcriptome sequencing raw data in this study have been deposited in the NCBI Gene Expression Omnibus (GEO) database under the accession number GSE284671 (https://www.ncbi.nlm.nih.gov/geo/query/acc.cgi?acc=GSE284671). And all data generated or analyzed during the current study are available from the corresponding author on reasonable request.

Declarations

Ethics approval and consent to participate

Animal welfare and experimental procedures were performed in accordance with the Guide for the Care and Use of Laboratory Animals (Ministry of Science and Technology of China, 2006) and were approved by the Animal Ethics Committee of Shenzhen University.

Consent for publication

Not applicable.

Competing interests

The authors declare no competing interests.

Author details

[1]Shenzhen Key Laboratory of Marine Bioresource & Eco-Environmental Science, College of Life Sciences and Oceanography, Shenzhen University, Shenzhen 518060, China
[2]Key Laboratory of Optoelectronic Devices and Systems of Ministry of Education and Guangdong Province, College of Physics and Optoelectronic Engineering, Shenzhen University, Shenzhen 518060, China
[3]Center for Plant Environmental Sensing, College of Life Sciences and Oceanography, Shenzhen University, Shenzhen 518060, China

Received: 8 January 2025 / Accepted: 18 April 2025
Published online: 02 May 2025

References

1. Hormsombut T, Mekjinda N, Kalasin S, Surareungchai W, Rijiravanich P. Mesoporous silica nanoparticles-enhanced microarray technology for highly sensitive simultaneous detection of multiplex foodborne pathogens. Acs Appl Bio Mater. 2024;7(4):2367–77. https://doi.org/10.1021/acsabm.4c00005.
2. Begić M, Josić D. Biofilm formation and extracellular microvesicles-the way of foodborne pathogens toward resistance. Electrophoresis. 2020;41(20):1718–39. https://doi.org/10.1002/elps.202000106.
3. Musa Moi I, Zuhairu I, Bashir MA, Yahaya MK, Auwal A, Gandi AY et al. Properties of foodborne pathogens and their diseases. Foodborne pathogens-recent advances in control and detection. IntechOpen. 2022. https://doi.org/10.5772/intechopen.105694
4. World Health Organization (WHO). Food safety. https://www.who.int/news-room/fact-sheets/detail/food-safety. Accessed 8 November 2023.
5. Daskalov H. The importance of *Aeromonas hydrophila* in food safety. Food Control. 2006;17(6):474–83. https://doi.org/10.1016/j.foodcont.2005.02.009.
6. Semwal A, Kumar A, Kumar N. A review on pathogenicity of *Aeromonas hydrophila* and their mitigation through medicinal herbs in aquaculture. Heliyon. 2023;9(3):e14088. https://doi.org/10.1016/j.heliyon.2023.e14088.
7. Wang J, Qin T, Chen K, Pan L, Xie J, Xi B. Antimicrobial and antivirulence activities of carvacrol against pathogenic *Aeromonas hydrophila*. Microorganisms. 2022;10(11):2170. https://doi.org/10.3390/microorganisms10112170.
8. Fiorentini C, Barbieri E, Falzano L, Matarrese P, Baffone W, Pianetti A, et al. Occurrence, diversity and pathogenicity of mesophilic *Aeromonas* in estuarine waters of the Italian Coast of the Adriatic sea. J Appl Microbiol. 2002;85(3):501–11. https://doi.org/10.1046/j.1365-2672.1998.853517.x.
9. Matyar F, Kaya A, Dinçer S. Distribution and antibacterial drug resistance of *Aeromonas* spp. From fresh and brackish waters in Southern Turkey. Ann Microbiol. 2007;57(3):443–7. https://doi.org/10.1007/bf03175087.
10. Stratev D, Odeyemi OA. Antimicrobial resistance of *Aeromonas hydrophila* isolated from different food sources: a mini-review. J Infect Public Heal. 2016;9(5):535–44. https://doi.org/10.1016/j.jiph.2015.10.006.
11. Rasmussen-Ivey CR, Figueras MJ, McGarey D, Liles MR. Virulence factors of *Aeromonas hydrophila*: in the wake of reclassification. Front Microbiol. 2016;7:1337. https://doi.org/10.3389/fmicb.2016.01337.
12. Talagrand-Reboul E, Jumas-Bilak E, Lamy B. The social life of *Aeromonas* through biofilm and quorum sensing systems. Front Microbiol. 2017;8:37. https://doi.org/10.3389/fmicb.2017.00037.
13. Lu L, Hu W, Tian Z, Yuan D, Yi G, Zhou Y, et al. Developing natural products as potential anti-biofilm agents. Chin Med. 2019;14(1):11. https://doi.org/10.1186/s13020-019-0232-2.
14. Yang M, Meng F, Gu W, Li F, Tao Y, Zhang Z, et al. Effects of natural products on bacterial communication and network-quorum sensing. Biomed Res Int. 2020;2020:1–10. https://doi.org/10.1155/2020/8638103.
15. Guo N, Bai X, Shen Y, Zhang T. Target-based screening for natural products against *Staphylococcus aureus* biofilms. Crit Rev Food Sci Nutr. 2021;63(14):2216–30. https://doi.org/10.1080/10408398.2021.1972280.
16. Abreu REF, Magalhães TC, Souza RC, Oliveira STL, Ibelli AMG, Demarqui FN, et al. Environmental factors on virulence of *Aeromonas hydrophila*. Aquac Int. 2017;26(2):495–507. https://doi.org/10.1007/s10499-017-0230-2.
17. John N, Vidyalakshmi VB, Hatha AAM. Effect of pH and salinity on the production of extracellular virulence factors by *Aeromonas* from food sources. J Food Sci. 2019;84(8):2250–5. https://doi.org/10.1111/1750-3841.14729.
18. Azad AK, Jensen KR, Lin CK. Coastal aquaculture development in Bangladesh: unsustainable and sustainable experiences. Environ Manage. 2009;44(4):800–9. https://doi.org/10.1007/s00267-009-9356-y.
19. Gentry RR, Froehlich HE, Grimm D, Kareiva P, Parke M, Rust M, et al. Mapping the global potential for marine aquaculture. Nat Ecol Evol. 2017;1(9):1317–24. https://doi.org/10.1038/s41559-017-0257-9.
20. Yi DL, Melnichenko O, Hacker P, Potemra J. Remote sensing of sea surface salinity variability in the South China sea. J Geophys Res Oceans. 2020;125(12). https://doi.org/10.1029/2020jc016827. e2020JC016827.
21. Su M, Liu N, Zhang Z, Zhang J. Osmoregulatory strategies of estuarine fish *Scatophagus argus* in response to environmental salinity changes. BMC Genomics. 2022;23(1):545. https://doi.org/10.1186/s12864-022-08784-2.
22. Chesney EJ, Baltz DM, Thomas RG. Louisiana estuarine and coastal fisheries and habitats: perspectives from a Fish's eye view. Ecol Appl. 2000;10(2):350–66. https://doi.org/10.1890/1051-0761(2000)010[0350:Leacfa]2.0.Co;2.
23. Nielsen UN, Wall DH, Adams BJ, Virginia RA, Ball BA, Gooseff MN, et al. The ecology of pulse events: insights from an extreme Climatic event in a Polar desert ecosystem. Ecosphere. 2012;3(2):1–15. https://doi.org/10.1890/es11-00325.1.
24. Kültz D, Podrabsky JE, Stillman JH, Tomanek L. Physiological mechanisms used by fish to Cope with salinity stress. J Exp Biol. 2015;218(12):1907–14. https://doi.org/10.1242/jeb.118695.
25. Chapman EJ, Byron CJ, Lasley-Rasher R, Lipsky C, Stevens JR, Peters R. Effects of climate change on coastal ecosystem food webs: implications for aquaculture. Mar Environ Res. 2020;162:105103. https://doi.org/10.1016/j.marenvres.2020.105103.
26. Sneed KE. Aquaculture: the farming and husbandry of freshwater and marine organisms. Prog Fish-Cult. 1973;35(3):184. https://doi.org/10.1577/1548-8659(1973)35[184:Afahof]2.0.Co;2.
27. Xie D, Chen F, Lin S, Wang S, You C, Monroig Ó, et al. Cloning, functional characterization and nutritional regulation of Δ6 fatty acyl desaturase in the herbivorous Euryhaline teleost *Scatophagus argus*. PLoS ONE. 2014;9(3):e90200. https://doi.org/10.1371/journal.pone.0090200.
28. Yang W, Wang Y, Jiang D, Tian C, Zhu C, Li G, et al. ddRADseq-assisted construction of a high-density SNP genetic map and QTL fine mapping for growth-related traits in the spotted scat (*Scatophagus argus*). BMC Genomics. 2020;21(1):278. https://doi.org/10.1186/s12864-020-6658-1.
29. Ghazilou A, Chenary F, Morovvati H, Zolgarneine H. Time course of saltwater adaptation in spotted scat (*Scatophagus argus*) (Pisces): A histomorphometric approach. Ital J Zool. 2011;78(1):82–9. https://doi.org/10.1080/11250003.2010.491099.
30. Jahid IK, Mizan MF, Ha AJ, Ha SD. Effect of salinity and incubation time of planktonic cells on biofilm formation, motility, Exoprotease production, and quorum sensing of *Aeromonas hydrophila*. Food Microbiol. 2015;49:142–51. https://doi.org/10.1016/j.fm.2015.01.016.
31. Lu M, Su M, Liu N, Zhang J. Effects of environmental salinity on the immune response of the coastal fish *Scatophagus argus* during bacterial infection. Fish Shellfish Immunol. 2022;124:401–10. https://doi.org/10.1016/j.fsi.2022.04.029.

32. Pianetti A, Battistelli M, Citterio B, Parlani C, Falcieri E, Bruscolini F. Morphological changes of *Aeromonas hydrophila* in response to osmotic stress. Micron. 2009;40(4):426–33. https://doi.org/10.1016/j.micron.2009.01.006.
33. Pianetti A, Manti A, Boi P, Citterio B, Sabatini L, Papa S, et al. Determination of viability of *Aeromonas hydrophila* in increasing concentrations of sodium chloride at different temperatures by flow cytometry and plate count technique. Int J Food Microbiol. 2008;127(3):252–60. https://doi.org/10.1016/j.ijfoodmicro.2008.07.024.
34. Bennett BM. Estimation of LD_{50} by moving averages. J Hyg (Lond). 2009;50(2):157–64. https://doi.org/10.1017/s0022172400019513.
35. O'Toole GA. Microtiter dish biofilm formation assay. J Vis Exp. 2011;47:e2437. https://doi.org/10.3791/2437.
36. Jahid IK, Lee NY, Kim A, Ha SD. Influence of glucose concentrations on biofilm formation, motility, Exoprotease production, and quorum sensing in *Aeromonas hydrophila*. J Food Prot. 2013;76(2):239–47. https://doi.org/10.4315/0362-028x.Jfp-12-321.
37. Truchado P, Gil-Izquierdo A, Tomás-Barberán F, Allende A. Inhibition by chestnut honey of N-Acyl-l-homoserine lactones and biofilm formation in Erwinia Carotovora, Yersinia Enterocolitica, and Aeromonas hydrophila. J Agric Food Chem. 2009;57(23):11186–93. https://doi.org/10.1021/jf9029139.
38. Robinson MD, McCarthy DJ, Smyth GK. EdgeR: a bioconductor package for differential expression analysis of digital gene expression data. Bioinformatics. 2010;26(1):139–40. https://doi.org/10.1093/bioinformatics/btp616.
39. Dong J, Zhang L, Liu Y, Zhou S, Yang Y, Xu N, et al. Resveratrol influences the pathogenesis of *Aeromonas hydrophila* by inhibiting production of Aerolysin and biofilm. Food Control. 2021;126:108083. https://doi.org/10.1016/j.foodcont.2021.108083.
40. Su M, Zhou J, Duan Z, Zhang J. Transcriptional analysis of renal dopamine-mediated Na^+ homeostasis response to environmental salinity stress in *Scatophagus argus*. BMC Genomics. 2019;20(1):418. https://doi.org/10.1186/s12864-019-5795-x.
41. Livak KJ, Schmittgen TD. Analysis of relative gene expression data using real-time quantitative PCR and the $2^{-\Delta\Delta CT}$ method. Methods. 2001;25(4):402–8. https://doi.org/10.1006/meth.2001.1262.
42. Natrah FMI, Alam MI, Pawar S, Harzevili AS, Nevejan N, Boon N, et al. The impact of quorum sensing on the virulence of *Aeromonas hydrophila* and *Aeromonas salmonicida* towards burbot (*Lota lota* L.) larvae. Vet Microbiol. 2012;159(1–2):77–82. https://doi.org/10.1016/j.vetmic.2012.03.014.
43. Zheng Q, Wang Y, Chen J, Li Y, Zhao F, Liu D, et al. Effects of salinity on the growth, physiological characteristics, and intestinal microbiota of the Echiura worm (*Urechis unicinctus*). Front Mar Sci. 2022;9:912023. https://doi.org/10.3389/fmars.2022.912023.
44. Sun S, Gong C, Deng C, Yu H, Zheng D, Wang L, et al. Effects of salinity stress on the growth performance, health status, and intestinal microbiota of juvenile *Micropterus salmoides*. Aquaculture. 2023;576:739888. https://doi.org/10.1016/j.aquaculture.2023.739888.
45. Conner JG, Teschler JK, Jones CJ, Yildiz FH, Kudva IT, Nicholson TL. Staying alive: vibrio Cholerae's cycle of environmental survival, transmission, and dissemination. Microbiol Spectr. 2016;4(2). https://doi.org/10.1128/microbiolspec.VMBF-0015-2015.
46. Vicente-Santos A, Willink B, Nowak K, Civitello DJ, Gillespie TR. Host-pathogen interactions under pressure: a review and meta-analysis of stress-mediated effects on disease dynamics. Ecol Lett. 2023;26(11):2003–20. https://doi.org/10.1111/ele.14319.
47. Barca AV, Vences A, Terceti MS, do Vale A, Osorio CR. Low salinity activates a virulence program in the generalist marine pathogen *Photobacterium damselae* subsp. *damselae*. mSystems. 2023;8(3):e0125322. https://doi.org/10.1128/msystems.01253-22
48. Palumbo SA, Morgan DR, Buchanan RL. Influence of temperature, NaCl, and pH on the growth of *Aeromonas hydrophila*. J Food Sci. 2006;50(5):1417–21. https://doi.org/10.1111/j.1365-2621.1985.tb10490.x.
49. Wang Y, Gu J. Influence of temperature, salinity and pH on the growth of environmental *Aeromonas* and *Vibrio* species isolated from Mai Po and the inner deep Bay nature reserve Ramsar site of Hong Kong. J Basic Microbiol. 2005;45(1):83–93. https://doi.org/10.1002/jobm.200410446.
50. Delamare APL, Costa SOP, Da Silveira MM, Echeverrigaray S. Growth of *Aeromonas* species on increasing concentrations of sodium chloride. Lett Appl Microbiol. 2000;30:57–60. https://doi.org/10.1046/j.1472-765x.2000.00662.x.
51. Ashikur RM, Akter S, Ashrafudoulla M, Anamul HCM, Uddin MAGMS, Hong PS, et al. Insights into the mechanisms and key factors influencing biofilm formation by *Aeromonas hydrophila* in the food industry: a comprehensive review and bibliometric analysis. Food Res Int. 2024;175:113671. https://doi.org/10.1016/j.foodres.2023.113671.
52. Li F, Xiong XS, Yang YY, Wang JJ, Wang MM, Tang JW, et al. Effects of NaCl concentrations on growth patterns, phenotypes associated with virulence, and energy metabolism in *Escherichia coli* BW25113. Front Microbiol. 2021;12:705326. https://doi.org/10.3389/fmicb.2021.705326.
53. Pridgeon JW, Yildirim-Aksoy M, Klesius PH, Kojima K, Mobley JA, Srivastava KK, et al. Identification of *GyrB* and *RpoB* gene mutations and differentially expressed proteins between a novobiocin-resistant *Aeromonas hydrophila* catfish vaccine strain and its virulent parent strain. Vet Microbiol. 2013;166(3–4):624–30. https://doi.org/10.1016/j.vetmic.2013.07.025.
54. Parsek MR, Singh PK. Bacterial biofilms: an emerging link to disease pathogenesis. Annu Rev Microbiol. 2003;57(1):677–701. https://doi.org/10.1146/annurev.micro.57.030502.090720.
55. Du H, Pang M, Dong Y, Wu Y, Wang N, Liu J, et al. Identification and characterization of an *Aeromonas hydrophila* oligopeptidase gene *PepF* negatively related to biofilm formation. Front Microbiol. 2016;7:1497. https://doi.org/10.3389/fmicb.2016.01497.
56. Wadhwa N, Berg HC. Bacterial motility: machinery and mechanisms. Nat Rev Microbiol. 2021;20(3):161–73. https://doi.org/10.1038/s41579-021-00626-4.
57. Li X, Yang B, Shi C, Wang H, Yu R, Li Q, et al. Synergistic interaction of low salinity stress with vibrio infection causes mass mortalities in the oyster by inducing host microflora imbalance and immune dysregulation. Front Immunol. 2022;13:859975. https://doi.org/10.3389/fimmu.2022.859975.
58. Fan Y, Evans CR, Ling J. Reduced protein synthesis fidelity inhibits flagellar biosynthesis and motility. Sci Rep. 2016;6(1):30960. https://doi.org/10.1038/srep30960.
59. Wilhelms M, Molero R, Shaw JG, Tomás JM, Merino S. Transcriptional hierarchy of *Aeromonas hydrophila* polar-flagellum genes. J Bacteriol. 2011;193(19):5179–90. https://doi.org/10.1128/jb.05355-11.
60. Canals R, Ramirez S, Vilches S, Horsburgh G, Shaw JG, Tomás JM, et al. Polar flagellum biogenesis in *Aeromonas hydrophila*. J Bacteriol. 2006;188(2):542–55. https://doi.org/10.1128/jb.188.2.542-555.2006.
61. Pemberton JM, Kidd SP, Schmidt R. Secreted enzymes of *Aeromonas*. FEMS Microbiol Lett. 1997;152(1):1–10. https://doi.org/10.1111/j.1574-6968.1997.tb10401.x.
62. Su Y, Wang C, Chen Y, Wang S, Shu C, Tsai P, et al. Haemolysin Ahh1 secreted from *Aeromonas Dhakensis* activates the NLRP3 inflammasome in macrophages and mediates severe soft tissue infection. Int Immunopharmacol. 2024;128:111478. https://doi.org/10.1016/j.intimp.2023.111478.
63. Jin L, Chen Y, Yang W, Qiao Z, Zhang X. Complete genome sequence of fish-pathogenic *Aeromonas hydrophila* HX-3 and a comparative analysis: insights into virulence factors and quorum sensing. Sci Rep. 2020;10(1):15479. https://doi.org/10.1038/s41598-020-72484-8.
64. Liu L, Yan Y, Feng L, Zhu J. Quorum sensing *AsaI* mutants affect spoilage phenotypes, motility, and biofilm formation in a marine fish isolate of *Aeromonas salmonicida*. Food Microbiol. 2018;76:40–51. https://doi.org/10.1016/j.fm.2018.04.009.
65. Simm R, Morr M, Kader A, Nimtz M, Römling U. GGDEF and EAL domains inversely regulate Cyclic di-GMP levels and transition from sessility to motility. Mol Microbiol. 2004;53(4):1123–34. https://doi.org/10.1111/j.1365-2958.2004.04206.x.

Publisher's note